technical notes Journal of proteome research

Measurement of Protein Phosphorylation Stoichiometry by Selected Reaction Monitoring Mass Spectrometry

Lily L. Jin,[†,‡,§] Jiefei Tong,[†,§] Amol Prakash,[||] Scott M. Peterman,[||] Jonathan R. St-Germain,[†,‡,§] Paul Taylor,[†,§] Suzanne Trudel,[⊥] and Michael F. Moran*[,†,‡,§]

McLaughlin Centre for Molecular Medicine, MaRS East Tower, 101 College Street, Toronto, M5G 1L7, Canada, Department of Molecular Genetics, and Banting and Best Department of Medical Research, University of Toronto, Toronto, Canada, Program in Molecular Structure and Function, The Hospital For Sick Children, Toronto, Canada, Biomarker Research Initiatives in Mass Spectrometry (BRIMS) Center, Thermo Fisher Scientific, Cambridge, Massachusetts 02139, and Hematology-Oncology, Princess Margaret Hospital and Ontario Cancer Institute, Toronto, Canada

Received January 12, 2010

Abstract: The stoichiometry of protein phosphorylation at specific amino acid sites may be used to infer on the significance of the modification, and its biological function in the cell. However, detection and quantification of phosphorylation stoichiometry in tissue remain a significant challenge. Here we describe a strategy for highly sensitive, label-free quantification of protein phosphorylation stoichiometry. Method development included the analysis of synthetic peptides in order to determine constants to relate the mass spectrometry signals of cognate peptide/phosphopeptide pairs, and the detection of the cognate peptides by using high resolution Fourier Transform mass spectrometry (FTMS) and selected reaction monitoring mass spectrometry (SRM). By analyzing extracted ion currents by FTMS, the phosphorylation stoichiometries of two tyrosine residues (tyrosine-194 and tyrosine-397) in the protein tyrosine kinase Lyn were determined in transfected human HEK293T cells and two cultured human multiple myeloma strains. To achieve high sensitivity to measure phosphorylation stoichiometry in tissue, SRM methods were developed and applied for the analysis of phosphorylation stoichiometries of Lyn phospho-sites in multiple myeloma xenograft tumors. Western immuno-blotting was used to verify mass spectrometry findings. The SRM method has potential applications in analyzing clinical samples wherein protein phosphorylation stoichiometries may represent important pharmacodynamic biomarkers.

Keywords: Label-free quantification • Lyn • Mass spectrometry • Phosphorylation • Multiple reaction monitoring MRM • Selected reaction monitoring SRM

Introduction

Protein phosphorylation is a universal mechanism of cell regulation, and inhibiting dysregulated kinases has been shown to be an effective therapeutic strategy to treat a growing list of cancers.[1] The quantitative measurement of phosphorylation stoichiometries in malignant tumors may reveal target kinases and signaling networks and can be used to guide drug discovery and development.[2] However, the measurement of protein phosphotyrosine (pY) is particularly challenging because it comprises only approximately 2% of protein phosphorylation, and often involves regulatory proteins expressed at low levels.[3]

Mass spectrometry (MS) is an effective tool to identify sites of protein phosphorylation, and has been extensively reviewed.[4,5] It can be unbiased (i.e., hypothesis free), therefore, requiring no previous knowledge of the cell system, enables the characterization of large numbers of phosphorylation sites,[2,6] and has been applied for the identification and quantification of drug-modulated phosphorylations in xenograft tumors.[7] Protein phosphorylation stoichiometry can be measured by MS,[8] but systematic analyses of protein phosphorylation stoichiometry have not been reported.

Label-free quantification of protein phosphorylation by MS is desirable since it has the potential to be applied to tissue samples (e.g., clinical tumor specimens) that are not amenable to metabolic labeling.[9] One method for label-free quantification involves the measurement of MS extracted ion currents (XICs) of analyte peptide ions, which are linearly related to quantity under constant experimental conditions.[10] Challenges in label-free quantification of protein phosphorylation include the requirement to match high confidence MS/MS-based peptide identifications with high resolution MS XICs,[11] biological variability in protein phosphorylation, and the low levels of protein expression and phosphorylation stoichiometries often associated with proteins involved in cell regulation.

Another approach for label-free, MS-based phospho-peptide quantification is selected reaction monitoring (SRM, also known as MRM, multiple reaction monitoring), in which specific precursor-to-product ion transitions are monitored during liquid chromatography (LC)−MS/MS in a triple quadrupole instrument.[12] This method allows the identification and quantification of peptide ions with high specificity in complex

* To whom correspondence should be addressed. Michael F. Moran, Phone: 647 235-6435. E-mail: m.moran@utoronto.ca, Address: 101 College St., East Tower, 9-804, Toronto, M5G 1L7, Canada.

† McLaughlin Centre for Molecular Medicine.

‡ University of Toronto.

§ Program in Molecular Structure and Function, The Hospital For Sick Children.

|| Biomarker Research Initiatives in Mass Spectrometry (BRIMS) Center, Thermo Fisher Scientific.

⊥ Princess Margaret Hospital and Ontario Cancer Institute.

10.1021/pr100024a

Published on Web 03/05/2010

mixtures,[6] and is an approach well established for the quantification of small molecules (e.g., drug metabolites and chemical synthesis intermediates).[13−17] LC−SRM effectively reduces background interference by targeting the analysis of specific peptides, making it a method of choice for measuring known phospho-peptides in complex peptide mixtures. Combined with label-based quantification strategies, it can be used to determine protein phosphorylation stoichiometry.[18−21]

Measuring protein phosphorylation stoichiometry by MS analysis of peptides requires the quantification of both the phosphorylated and corresponding nonphosphorylated peptides. However, cognate peptide pairs typically display distinctly different LC and mass spectrometric properties.[22] Therefore, factors must be predetermined for each peptide/phosphopeptide pair in order to relate their values and calculate relative abundances and stoichiometry.[8] Such correction factors are unique to each peptide/phosphopeptide pair and remain constant under controlled experimental conditions. As demonstrated by Steen et al.,[8] the quantitative conversion of a phosphopeptide to its cognate peptide by phosphatase treatment is one method to generate and compare equimolar samples of cognate modified/unmodified peptides prior to MS analysis for the determination of such factors. Indeed, phosphatases have been used to aid the identification and quantification of protein phosphorylation by MS.[8,13,23,24]

To develop a method to quantify protein phosphorylation stoichiometry in tumors, we undertook to combine LC−SRM with label-free quantification. Lyn is the predominant Src family protein-tyrosine kinase in B cells and implicated in B cell related malignancies including multiple myeloma (MM).[25] We examined in MM-derived cells and tumors the Lyn kinase at two phosphorylation sites, Y397 and Y194. Phosphorylation at Lyn residue Y397 in the kinase domain activation loop is associated with the activation of intrinsic kinase activity.[25] Lyn residue Y194 resides in the SH2 domain and is uncharacterized. Phosphorylation of the analogous residue in Src was found to modulate autoregulatory, intramolecular interactions of the SH2 domain that regulate kinase domain activation.[26] Hence, the modification of Lyn residues Y397 and Y194 are associated with mechanistically defined effects on Lyn activity. Therefore, we undertook to measure the stoichiometry of phosphorylation at these positions.

Both sites in Lyn were found amenable to proteomics studies, and their phosphorylation stoichiometries were measured. The label-free method we describe here may have general utility for phospho-proteomics studies including the measurement of signaling pathways in clinical samples and preclinical models.

Materials and Methods

Antibodies, Enzymes, and DNA Constructs. For immunoprecipitation (IP), agarose-conjugated anti-Lyn mouse antibody was obtained from Santa Cruz Biotechnology (Santa Cruz, CA). Anti-pY antibody (anti-pTyr-100, PhosphoScan Kit) for phospho-peptide purification was from Cell Signaling Technology (Danvers, MA). For Western blotting, anti-Lyn rabbit antibody and phospho-Src family (Tyr416) antibody were obtained from AbD Serotec (Oxford, U.K.), and Cell Signaling Technology, respectively. Peptides with sequences SLDNGGYpYISPR and VIEDNEpYTAR (human Lyn residues 187−198 and 392−400, respectively) were custom-made by the Advanced Protein Technology Centre (The Hospital For Sick Children, Toronto). Sequence verified full-length human Lyn cDNA encoding C-terminal V5 and N-terminal GST were cloned into the mammalian expression vector pcDNA40 (pcDNA40-Lyn-V5) and the bacterial expression vector pDEST15 (Invitrogen, Carlsbad, CA) (pDEST15-GST-Lyn). Full-length phosphotyrosine phosphatase 1B (PTP1B) encoding N-terminal GST tag cloned into a pGEX expression vector was a gift from Dr. Benjamin Neel (Ontario Cancer Institute, Toronto, Ontario). All other chemical reagents were purchased from Sigma Aldrich (St. Louis, MO), and aqueous solutions were prepared using Milli-Q grade water (Millipore, Bedford, MA).

Cell Lines, Cell Culture, And Xenograft Tumors. Human embryonic kidney 293T (HEK293T) cells were maintained in Dulbecco's Modified Eagle Medium with 10% fetal bovine serum (FBS) supplemented with nonessential amino acids. Human MM cell lines Kawasaki Medical School (KMS) 11 and KMS12 pleural effusion were maintained in Iscove's Modified Dulbecco's Media with 10% FBS. Four- to 8-week-old male nonobese diabetic/severe combined immunodeficiency mice were inoculated subcutaneously with 10^7 KMS12 cells in 200 μL of 50% matrigel basement membrane matrix (DB, Franklin Lakes, NJ). Animals were sacrificed when tumors reached 1 cm. Harvested tumors were immediately frozen on dry ice and stored at −70 °C.

Treatment of Cells with Pervanadate. Equal volumes of 12 mM Na_3VO_4 and 12 mM H_2O_2 were mixed, and after 15 min diluted 1:100 into subconfluent cultures of MM cells, or HEK293T cells 40−48 h post-transfection. The cells were incubated at 37 °C for 15 min and then collected.

Cell and Tissue Lysis. Cultured KMS11 or KMS12 cells were collected by low-speed centrifugation, washed with phosphate buffered saline (PBS) pH 7, resuspended in cell lysis buffer (0.01 M sodium phosphate pH 7.2, 0.15 M NaCl, 1% Triton X-100, 1% sodium deoxycholate, 0.1% sodium dodecyl sulfate, 2.5 mM ethylenediaminetetraacetic acid, 0.05 M sodium fluoride), and inverted at 4 °C for 30 min. KMS12 tumor lysate was obtained by briefly homogenizing KMS12 xenograft tumors in cell lysis buffer followed by inverting at 4 °C for 30 min. Lysates were centrifuged at 15 000*g* at 4 °C for 10 min to remove insoluble material. For MS analysis, the supernatants were further clarified by ultracentrifugation for 60 min at 100 000*g*. Cell-free lysates were quantified for protein concentration and analyzed by protein or peptide IP (following trypsin digestion) and/or Western blotting essentially as described previously.[27]

Peptide Dephosphorylation. For GST Lyn derived peptides, 1 u of Calf Intestinal Alkaline Phosphatase (CIAP, Fermentas, Vilnius, Lithuania) was added to a 25-mM pervanadate solution containing 0.5 mM pY and 10−30 fmol GST Lyn derived peptides, and incubated for 5, 30, or 60 s at 37 °C. The solution was acidified to 1% TFA and incubated on ice to inhibit the phosphatase. For complete dephosphorylation of synthetic peptides, 150 fmol peptide was mixed with 1 u CIAP in 25 mM NH_4HCO_3 and incubated at 37 °C for 60 s. For controlled partial dephosphorylation, 1 pmol peptide was incubated with 0−1.5 u PTP1B at 37 °C for 1 h in Tris buffer (50 mM Tris.HCl, 0.15 M NaCl, pH 7). The reaction was stopped by adjusting to a final concentration of 0.5% TFA and 1 mM Na_3VO_4. The peptides were desalted by mini-scale purification, as described below.

Peptide Desalting. For standard-scale purification (100−500 μg of peptide), C-18 chromatography was performed as previously described.[27] For mini-scale purification (<5 μg of peptide), C-18 ZipTips were used according to manufacturer's protocol

(Eppendorf AG, Hamburg). The eluted peptides were dried by centrifugation under vacuum (SpeedVac).

Analysis by LC−MS/MS. Peptide mixtures were dissolved in 0.1% formic acid and automatically loaded onto a homemade C-18 precolumn for concentrating and desalting at 5 μL/min. The peptides were resolved by reverse-phase chromatography on a nanoliter-scale LC system (Easy-nLC, Proxeon Biosystems A/S, Odense, Denmark) coupled with an LTQ-Orbitrap mass spectrometer (Thermo Scientific), and were eluted by using a linear gradient 0−35% buffer B (5% H_2O, 95% acetonitrile, 0.1% formic acid in HPLC water) over 120 min at 250 nL/min. Data were acquired by coupling a high resolution MS scan (m/z range 400−1400) in the Orbitrap with 3 MS/MS scans in the LTQ, generated by collision-induced dissociation (CID). The m/z values selected for MS/MS were dynamically excluded for 30 s.

Assigning Peptide Sequences Using SEQUEST and X! Tandem Algorithms. Tandem mass spectra were extracted by BioWorks version 3.3 (Thermo Fisher Scientific) and searched using SEQUEST (Thermo; version 27, rev. 12) and X! Tandem[28] (www.thegpm.org; version 2006.04.01.2). Both were set to search against the international protein index (IPI) Human database (v3.29, downloaded from ftp.ebi.ac.uk/pub/databases/IPI, 68 161 protein entries), assuming trypsin digestion while allowing 2 missed cleavages, with a fragment ion mass tolerance of 0.5 Da and a parent ion tolerance of 0.02 Da. The iodoacetamide derivative of cysteine was specified in SEQUEST and X! Tandem as a fixed modification. Phosphorylation of tyrosine in SEQUEST and phosphorylation of tyrosine, serine, and threonine in X! Tandem were specified as variable modifications. The oxidation of methionine was also specified as a variable modification in both search engines.

Measurement of Extracted Ion Current (XIC). For LC−MS/MS, the XIC of a peptide ion was extracted by specifying its m/z in Xcalibur software (Thermo Scientific, Version 2.0.7), while applying the curve smoothing function with BoxCar = 3. XIC peak areas were determined with the Toggle Peak Detection function of Xcalibur with default settings. For automatic determination, the raw data file was converted into mzXML format by ReAdW, searched by X! Tandem, then converted into pepXML format by Tandem2XML. Both ReAdW and Tandem2XML were downloaded as part of the trans proteomic pipeline (TPP) (tools.proteomecenter.org/wiki/index.php?title=Software:TPP, version 3.3.0). Both the mzXML and pepXML files were analyzed by using SuperHirn software (Version 0.04),[29] with an MS1 retention time tolerance of 1 min, an MS1 m/z tolerance of 0.02 Da, an MS2 m/z tolerance of 0.5 Da, and an MS1 feature CHRG range min of 2. The SuperHirn program default values were used for the rest of the parameters.

Peptide Analysis and Quantification by LC−SRM. Peptide mixtures were loaded onto the precolumn as described above and eluted using a linear gradient 0−60% HPLC buffer B over 40 min at 400 nL/min. The peptides were analyzed by positive ion nanoelectrospray ionization (ESI) LC−SRM on a TSQ Quantum Ultra triple quadrupole mass spectrometer (Thermo Scientific). The instrument was set to cycle through all 63 transitions (20 ms each) for a total cycle time of approximately 1.8 s, at a scan width of 0.01, by using resolution of 0.4 Da at full width at half-maximum in Q1 and 0.7 Da in Q3. The collision energy, calculated by using the formula 3.41 + 0.034 × (m/z of parent peptide), with collision gas pressure at 1.5 mTorr, was applied to fragment the parent peptides.[30]

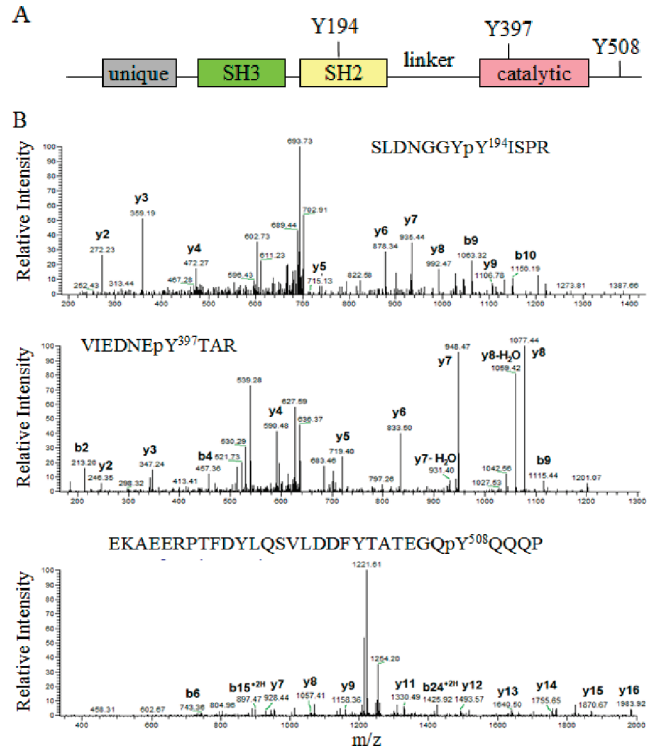

Figure 1. Lyn peptides corresponding to tyrosine phosphorylation sites were detected by LC−MS/MS in a multiple myeloma xenograft tumor. (A) Schematic drawing of the protein tyrosine kinase Lyn including three sites of tyrosine phosphorylation implicated in the regulation of kinase activity. (B) LC−MS/MS analysis of Lyn phosphotyrosine-containing peptides isolated from a multiple myeloma KMS12 xenograft tumor. Upper panel pY194 peptide (X! Tandem score: 3.51); Middle panel pY397 peptide (X! Tandem score: 6.11); lower panel pY508 peptide (X! Tandem score: 5.66). Certain y and b ions are labeled.

For SRM method development and optimization, transitions were initially selected according to maximum magnitude displayed during MS/MS in the LTQ-Orbitrap, and then optimized empirically in order to achieve maximum summed transition intensities in the triple quadrupole instrument (Thermo, TSQ Quantum Ultra). Identical nano-HPLC conditions were used with the two different MS platforms in order to maintain consistent peptide elution times. SRM signals were verified by manual inspection and confirmation of coelution of all associated transitions by using Xcalibur software. To further verify the specificity of SRM methods for peptide identification, synthetic Lyn peptides were spiked into whole cell trypsin digests and analyzed by LC−SRM. For each target peptide, only a single major peak was observed. Peak areas were determined with the Toggle Peak Detection function of Xcalibur with default settings, while applying the curve smoothing function with BoxCar = 3.

Results

Lyn Phosphorylation at Three Tyrosine Sites in Multiple Myeloma Tumor Tissue. The protein tyrosine kinase Lyn has been implicated as activated in MM.[31] Src family kinases such as Lyn are subject to complex regulation involving phosphorylation within their catalytic and carboxyl-terminal domains (Figure 1A),[32] and, we speculate, at a conserved tyrosine located in the SH2 domain.[26] Analysis of MM cell and xenograft tissue

Table 1. Transitions of Lyn-Derived Peptides Monitored by SRM

Lyn tryptic peptide	protein sequence numbers	transition $[MH]^+ > m/z$	ion
QQRPVPESQLLPGQR	41−55	578.32 > 457.25	y4
		578.32 > 898.51	y8
		578.32 > 1320.73	y12
VLEEHGEWWK	92−101	656.82 > 842.39	y6
		656.82 > 1100.57	y8
QLLAPGNSAGAFLIR	142−156	764.44 > 1102.6	y11
		764.44 > 1173.64	y12
		764.44 > 1286.72	y13
GSFSLSVR	163−170	426.73 > 474.3	y4
		426.73 > 561.34	y5
		426.73 > 474.3	y6
DFDPVHGDVIK	171−181	621.31 > 668.4	y6
		621.31 > 864.55	y8
SLDNGGYYISPR	187−198	671.33 > 912.46	y8
		671.33 > 1026.5	y9
		671.33 > 1141.53	y10
SLDNGGYpY^{194}ISPR	187−198	711.31 > 472.25	y4
		711.31 > 715.28	y5
		711.31 > 878.34	y6
		711.31 > 935.44	y7
		711.31 > 992.47	y8
		711.31 > 1106.51	y9
		711.31 > 1221.54	y10
SLDNGGpY^{193}YISPR	187−198	711.31 > 635.35	y5
SLDNGGpY^{193}pY^{194}ISPR	187−198	751.29 > 472.29	y4
		751.29 > 715.32	y5
		751.29 > 958.35	y6
		751.29 > 1015.37	y7
		751.29 > 1072.39	y8
		751.29 > 1186.43	y9
GSLLDFLK	325−332	446.76 > 635.57	y5
		446.76 > 748.5	y6
IADFGLAR	383−390	431.74 > 563.3	y5
		431.74 > 678.43	y6
VIEDNEYTAR	391−400	605.29 > 347.2	y3
		605.29 > 510.27	y4
		605.29 > 753.35	y6
		605.29 > 868.38	y7
		605.29 > 997.42	y8
VIEDNEpY^{397}TAR	391−400	645.27 > 590.23	y4
		645.27 > 833.3	y6
		645.27 > 948.35	y7
		645.27 > 1059.38	y8-H_2O
		645.27 > 1077.39	y8
VIEDNEYpT^{398}AR	391−400	645.27 > 596.29	precursor-98

samples following phosphopeptide enrichment[33] indicated the phosphorylation of these three tyrosine residues in Lyn (Y194, Y397, Y508) (Figure 1B). However, these data do not provide insight into the extent, or stoichiometry, of these modifications, which is essential in order to assess the activation state of Lyn.

Normalization and Calculation of Response Rate Ratios. To facilitate the measurement of Lyn phosphorylation stoichiometry at Y194 and Y397, both of which are implicated in the activation of Lyn activity, the relative MS response rates of the Y194 and Y397 peptides with and without phosphorylation modifications were determined essentially by using the strategy of Steen et al.[8] The negative regulatory phosphorylation at position Y508 was not readily amenable to analysis in trypsin-digested samples and was not included in this study.

First, we established that the linear range of label-free quantification of 7 Lyn-derived peptides (SI Table 1) by Orbitrap Fourier Transform MS (XIC peak areas) and by SRM analysis (see Table 1 for transitions) on a TSQ triple quadrupole instrument spanned at least 3 orders of magnitude (0.5 fmol to 1 pmol) (Figure 2, SI Figure 1). We restricted our subsequent quantification analyses within this range.

Next, we determined the response rate ratios of cognate peptide pairs corresponding to the two Lyn phosphorylation sites described above. Synthetic peptides biochemically identical to the Lyn-derived tryptic peptides containing Y194 or Y397 (Lyn residues 187−198 and 392−400, respectively), in phosphorylated and unphosphorylated isoforms, were mixed at known molar ratios. The mixtures were analyzed by LC−MS and the peak areas of their corresponding XICs were determined (Figure 3A,B). Response rates were calculated by dividing the XIC values by quantity. In both cases, the Y-containing peptide had a higher response rate than the corresponding phosphorylated peptide. Response rate ratios (i.e., Y-peptide response rate/pY-peptide response rate) were then derived.

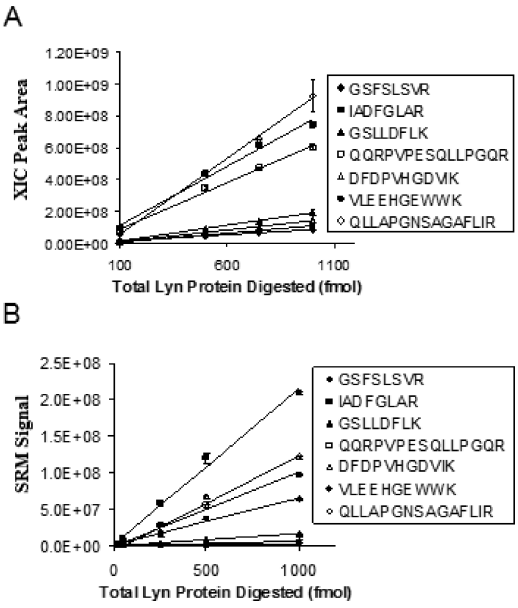

Figure 2. MS XIC peak areas and SRM signals of Lyn peptides are linearly related to quantity. (A) xy plot of MS XIC peak areas (*y*-axis) of 7 Lyn-derived peptides (labeled by sequences; see Table 1 for corresponding Lyn residue numbers) analyzed by Fourier transform MS versus quantities of the peptides (*x*-axis). (B) xy plot of SRM signals of Lyn-derived peptides (*y*-axis) analyzed by LC-SRM versus quantities of the peptides (*x*-axis). Fitted linear trendlines are shown for both graphs. Error bars denote standard deviations in 2 technical repeats.

Values (mean ± SD, $n = 3$) of 1.08 (±0.03) and 1.87 (±0.59) were determined for the Y194/pY194 and Y397/pY397 pairs, respectively. These values were used in subsequent analyses of stoichiometry in order to equate the values obtained for the cognate phospho- and nonphospho-peptides.

To establish a normalization scheme for Lyn, GST-Lyn protein was purified from bacteria and subjected to trypsin digestion and LC−MS/MS analysis (see Materials and Methods). Three Lyn peptides (QQRPVPESQLLPGQR, residues 41−55; QLLAPGNSAGAFLIR, residues 142−156; and GSFSLSVR, residues 163−170) consistently yielded good response rates in every sample, and were analyzed for candidacy as normalization peptides. Two of the three were accepted as good normalization peptides by using criteria described in Steen et al.[8] and explained in Supplementary Methods (SI Figure 3), and were used to normalize the quantification results across samples.

To test Lyn phosphorylation stoichiometry measurement, cells expressing relatively high levels of Lyn protein were established and treated with the protein-pY phosphatase inhibitor pervanadate to generally potentiate protein pY levels. A mammalian expression vector encoding human Lyn was transfected into HEK293T cells. At 48 h post-transfection, the cells were treated with or without pervanadate and then lysed (see Materials and Methods). The whole cell lysates (700 μg of protein per sample) were subjected to immunoprecipitation (IP) with anti-Lyn and the lysate and IP samples were then analyzed by Western (immuno) blotting (Figure 3C), and including GST Lyn standards (Figure 3C, lanes 1−3) to facilitate quantification of Lyn expression and recovery. The Lyn protein copy number per cell was calculated to be approximately 8.4×10^5. A total of 163 ng (~3 pmol) Lyn protein per sample was analyzed by LC−MS/MS. The peptides containing the Y194 and Y397 sites with or without phosphorylation were identified by

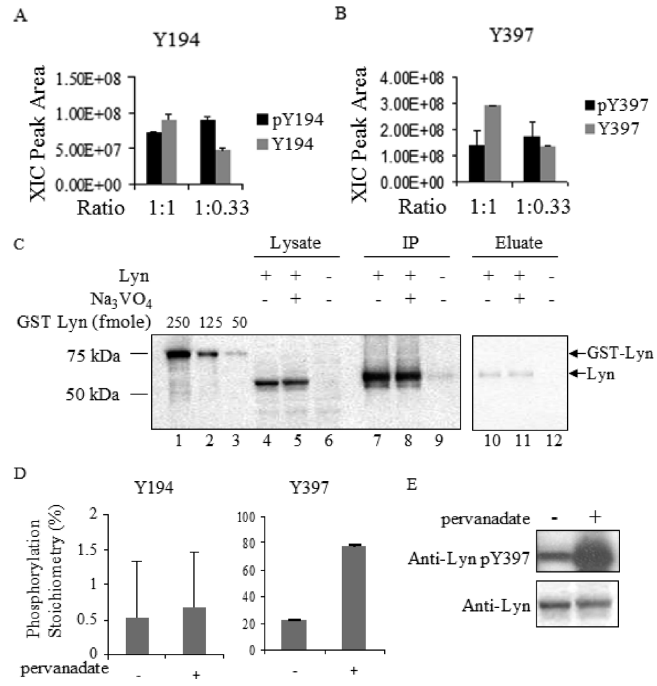

Figure 3. Determination of the in vivo phosphorylation stoichiometry of Lyn in HEK293T cells. (A and B) Bar graphs of the XIC peak areas of pY194/Y194 (A) and pY397/Y397 (B) associated Lyn tryptic peptides mixed at different molar ratios and analyzed by LC−MS. Labels of *x*-axis represent the molar ratio of pY (black) to Y (gray) peptide mixtures. Error bars denote standard deviation of 3 technical repeats. The average response rate ratios were determined to be 1.08 and 1.87 for the Y194 and Y397 associated peptides, respectively. (C) Anti-Lyn blot of HEK293T cell lysates and Lyn enriched fractions. HEK293T cells transfected with a recombinant Lyn construct, treated with (lanes 5, 8, 11) or without (lanes 4, 7, 10) pervanadate, were lysed, and the total protein extracts (700 μg) were immunoprecipitated for Lyn. The antibody-conjugated beads were eluted with 8 M urea and the eluate was protease digested and analyzed by MS. The lysate (10 μg) (lanes 4−6), 1/10 of the immunoprecipitated fractions (lanes 7−9), and 1/50 of the total eluted fractions (lanes 10−12) were loaded on gel. Lanes 6, 9, and 12 correspond to samples from untransfected HEK293T cells prepared as described. GST Lyn proteins (lanes 1−3) were loaded as reference. Molecular weight markers are shown on the left. (D) Phosphorylation stoichiometry of Lyn Y194 or Y397 sites in transfected HEK293T cells, treated with or without pervanadate, were determined by LC−MS. Error bars denote standard errors of stoichiometry determination in transfected HEK293T cells ($n = 3$). (E) Lysate (10 μg) from Lyn transfected HEK293T cells were blotted with an antibody directed against pY397 (top) and anti-Lyn antibody (bottom).

MS/MS. Their MS XIC peak areas were determined and used to calculate phosphorylation stoichiometry by using eq 1. In control and pervanadate-treated cells, the respective phosphorylation stoichiometries were calculated to be 0.53% and 0.67% at Y194, and 21.9% and 77.7% at Y397 (Figure 3D). The approximately 3.5-fold increase in phosphorylation stoichiometry at Y397 was highly significant ($p < 0.0001$), whereas the slight increase in phosphorylation stoichiometry at Y194 was not ($p = 0.9773$). To verify this result, Lyn Y397 phosphorylation and total Lyn levels in the samples were examined by Western blotting. The chemiluminescence signal of pY397 in the pervanadate-treated sample compared with sample from untreated cells was increased 2.5-fold, but only a minor change in total Lyn level was observed (Figure 3E). This was consistent

with the MS results. The phosphorylation level of Y194 was not determined by Western immuno-blotting because pY194-specific antibodies were not commercially available. These experiments indicated that the phosphorylation stoichiometry of ectopically expressed Lyn could be measured by MS, and that the stoichiometry of phosphorylation and sensitivity to pervanadate treatment is greater at position Y397 than Y194.

$$\frac{\text{[XIC pY peptide]}}{\text{[XIC pY peptide]} + \text{[XIC Y peptide]} / \text{[response rate ratio]}} \quad (1)$$

Measurement of Endogenous Lyn Phosphorylation Stoichiometry by LC−MS in Multiple Myeloma Cells. After showing that the phosphorylation stoichiometry of ectopically expressed Lyn was measurable, we verified that endogenous Lyn was phosphorylated at Y397 and Y194 in MM cell lines, and determined the phosphorylation stoichiometry at these sites. KMS11 and KMS12 are two human MM-derived cell lines that express Lyn. Detection of cognate Lyn-derived peptide/phosphopeptide pairs by MS is more difficult for these cells because Lyn is expressed at endogenous levels that are approximately 1/20 that observed in the transfected HEK293T system (described above). Therefore, extra enrichment steps were carried out in order to facilitate the detection of pY-containing Lyn peptides by MS. The tandem IP method of Tong et al.,[27] which involves the extraction of pY-containing peptides from trypsin-digested immune complexes, was used. Lyn proteins were isolated by anti-Lyn IP from KMS11 and KMS12 cells that had been treated with or without pervanadate. The IP samples were digested with trypsin and analyzed by Western blotting (Figure 4A). This confirmed the efficient recovery of Lyn from both cell types (see the Lyn-depleted lysates in lanes 5 and 6), and complete Lyn digestion by trypsin (lanes 9 and 10). The digested peptides were subjected to a second round of immunoprecipitation involving anti-pY. Both the pY-enriched and the flow-through fractions from the second IP were analyzed by LC−MS/MS. The XIC peak areas of identified Lyn peptides were quantified by using SuperHirn software.[29] Of the 22 non-pY-containing Lyn peptides identified, 3 (GSFSLSVR, residues 163−170; LGAGQFGEVWMGYYNNSTK, residues 251−271; and WTAPEAINFGCFTIK, residues 409−423) showed moderate to high degrees (40−90%) of nonspecific binding to the pY antibody, while the other 19 were almost exclusively found in the flow-through fraction. All of the Lyn pY194 peptide and the majority of the pY397 peptide (>91%) were detected in the anti-pY-enriched fraction. The distribution of the phospho- and nonphospho-peptides shows the specificity of the tandem IP of pY (TIPY)-MS method for targeted analysis of pY-containing peptides.[27] XIC peak areas from both fractions were measured and used to derive phosphorylation stoichiometries by using the response rate ratios of 1.08 and 1.87 (see previous section). In untreated and pervanadate treated KMS11, Y397 phosphorylation stoichiometries were 2.24% and 58.6%, respectively; in untreated and pervanadate treated KMS12, the respective values were 0.7% and 90.4%. In both cases, the pervanadate-induced changes in phosphorylation stoichiometry were highly significant ($p < 0.0001$). The Y194 peptide was detected in all KMS11 and KMS12 samples (with or without pervanadate), but the pY194 peptide was not detected above background levels in KMS11 or untreated KMS12 samples. Phosphorylation at this site was measured to be 9.2% in pervanadate-treated KMS12 cells (p-value <0.0001) (Figure 4B). Therefore, the basal level of pY194 was below our level of detection in the myeloma cell types.

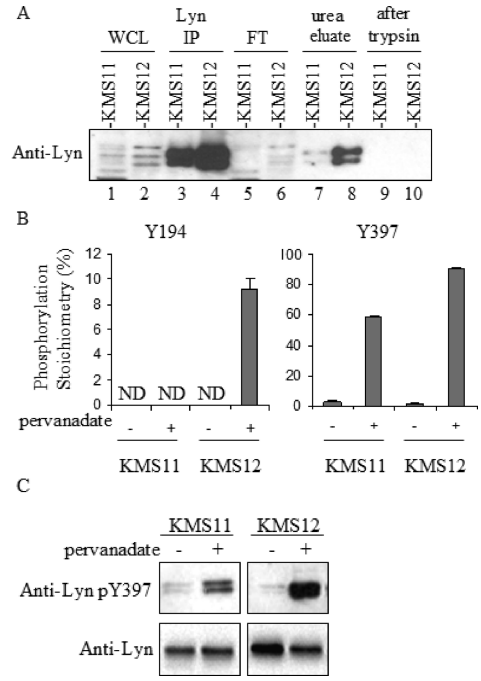

Figure 4. Determination of the in vivo phosphorylation stoichiometry of Lyn in multiple myeloma cells. (A) Anti-Lyn blot of MM cell lysates and Lyn enriched fractions. KMS11 and KMS12 cells were lysed and enriched for Lyn by immunoprecipitation (IP). Cell lysate (10 μg; lanes 1, 2), depleted lysate after Lyn IP (lanes 5, 6), 1/10 of the anti-Lyn IP fraction (lanes 3, 4), 1/50 of the urea eluate of the Lyn IP fractions (lanes 7, 8), and eluted fractions after trypsin digestion (lanes 9, 10) were blotted with anti-Lyn antibody. Trypsin-digested Lyn IPs were extracted with anti-pY, and the IP and flow through fractions were analyzed by LC−MS/MS. MS extracted ion currents (XICs) were quantified to determine phosphorylation stoichiometries (see Materials and Methods). (B) Bar graphs of Lyn Y194 and Y397 phosphorylation stoichiometry in KMS11 and KMS12 cells. In all cases, the nonphosphorylated Y194 and Y397 peptides were detected, but in the two KMS11 samples and untreated KMS12 sample, the pY194 peptide XIC was not detected above background and consequently stoichiometry was not determined (ND), as indicated. Error bars indicate standard deviation of phosphorylation stoichiometry ($n = 3$). (C) Lysate (10 μg) of KMS11 or KMS12 cells, treated with or without pervanadate, were blotted with an antibody directed against pY397 (top) and anti-Lyn antibody (bottom).

The amounts of Lyn protein and Y397 phosphorylation were examined in KMS11 and KMS12 cells by Western immunoblotting (Figure 4C). While only moderate changes were observed for the total Lyn level in pervanadate treated or untreated cells, pY397 levels were dramatically increased in both pervanadate-treated cell lines. The increase in pY397 levels was more pronounced in KMS12 cells (124-fold) as compared to KMS11 cells (approximately 20-fold). These trends and values agree with the MS-based quantification of pY397, which showed a more pronounced increase in KMS12 cells (approximately 129-fold) as compared to KMS11 cells (approximately 26-fold).

On the basis of these results, the TIPY tandem IP method (anti-Lyn → trypsin → anti-pY)[27] was confirmed as a sensitive

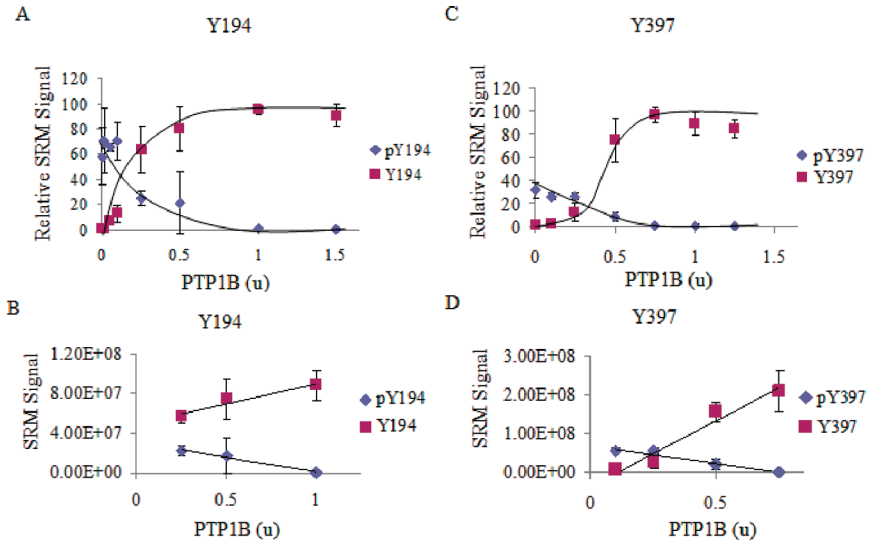

Figure 5. Determination of response rate ratios of cognate Lyn pY/Y peptides by LC−SRM. (A) Line graph of the SRM signals (summed from SRM transitions listed in Table 1) of synthetic peptides, biochemically identical to the Lyn pY194-containing tryptic peptide (pY194) and its dephosphorylated cognate (Y194). The phospho-peptides were treated with increasing concentrations of phosphotyrosine phosphatase 1B (PTP1B) at 37 °C for 1 h and analyzed by LC−SRM. (B) SRM signal versus PTP1B concentration were plotted for the cognate peptide pair for subsaturation concentrations of PTP1B. Fitted linear trendlines are shown. Panels C and D are results for synthetic peptides corresponding to Lyn pY397-containing tryptic peptide (see transitions in Table 1). Error bars indicate standard deviations ($n = 3$). The response rate ratios of the cognate Y194 and Y397-containing peptide pairs were calculated as a ratio of the slopes (eq 2) and determined to be 1.33 and 3.33, respectively.

method for the quantification of low-abundance phosphopeptides. However, because the pY-enriched and flow-through fractions were physically separated and differentially processed prior to MS analysis, they may be subjected to varying degrees of loss as a source of error. To overcome this limitation, an LC−SRM method was developed and applied as an alternative strategy. The ability of LC−SRM to target the analysis of low-abundance molecules in a complex mixture eliminated the requirement for the physical separation of pY peptides from the Y peptides, potentially generating more accurate and reproducible results.

Phosphorylation Stoichiometry Measurement by LC−SRM. Lyn-derived peptides and phosphopeptides were targeted for LC−SRM. We first experimentally optimized the (precursor → product) ion transitions used for quantifying Lyn-derived target peptides (Table 1). Each peptide was quantified by using the summed SRM signals of its transitions. We then determined the response rate ratios for cognate (phospho and nonphospho) peptide pairs containing Y194 and Y397 by using these transitions, which were also used in all subsequent experiments.

To determine the response rate ratios, purified recombinant PTP1B was used to dephosphorylate synthetic Lyn phosphopeptides. Synthetic peptides biochemically identical to the Lyn-derived tryptic peptides containing pY194 or pY397 were incubated with increasing concentrations of PTP1B for 1 h and then analyzed by LC−SRM. For each peptide, SRM signals (summed for the transitions listed in Table 1) were plotted against the concentration of PTP1B (Figure 5A,C). At subsaturation levels, the changes in peptide quantities are linearly related to the PTP1B concentrations (Figure 5B,D). Because of the substrate → product relationship between each phosphopeptide and cognate nonphosphorylated peptide, the observed decrease in the amount of each phospho-peptide was accompanied by a reciprocal, equimolar accumulation of the cognate nonphosphorylated peptide. Consequently, the response rate ratio was calculated as the ratio of the change rates, or slopes (eq 2), fitted by using only the data points at subsaturation concentrations. The calculated SRM response rate ratios (i.e., Y-peptide/pY-peptide) for cognate peptide pairs corresponding to Y194 and Y397 sites were 1.33 and 3.33, respectively.

$$\text{Response rate ratio} = \frac{[\text{slope of the increase of SRM signal of Y peptide}]}{[\text{slope of the decrease of SRM signal of pY peptide}]} \quad (2)$$

To further test this approach, GST-Lyn fusion protein was purified from bacteria, and following digestion with trypsin, peptides were incubated with PTP1B (as indicated, Figure 6) and then analyzed by LC−SRM. The SRM signals of cognate peptide pairs corresponding to Y194 and Y397 sites, normalized and averaged from two technical repeats, were plotted for the four time points (Figure 6A−D). The signals from the phosphopeptides decreased as the treatment time increased, consistent with dephosphorylation. The signals associated with the corresponding unphosphorylated peptides did not show significant increase. These observations indicated that with the bacterially expressed protein the phosphorylation stoichiometries at these sites were relatively low.

Next, the phosphorylation stoichiometries were calculated by using eq 1 and plotted against the four time points (Figure 6E,F). The measured phosphorylation stoichiometries decreased during the dephosphorylation reactions as expected. The rates of dephosphorylation at the two sites were clearly different (compare Figure 6, panels E and F). The Y397 site was completely dephosphorylated within 30 s, while the Y194 site was still phosphorylated to a level of 25% of the untreated amount after 60 s. Before PTP1B treatment, the phosphorylation stoichiometry of GST Lyn at Y397 was greater than 10%,

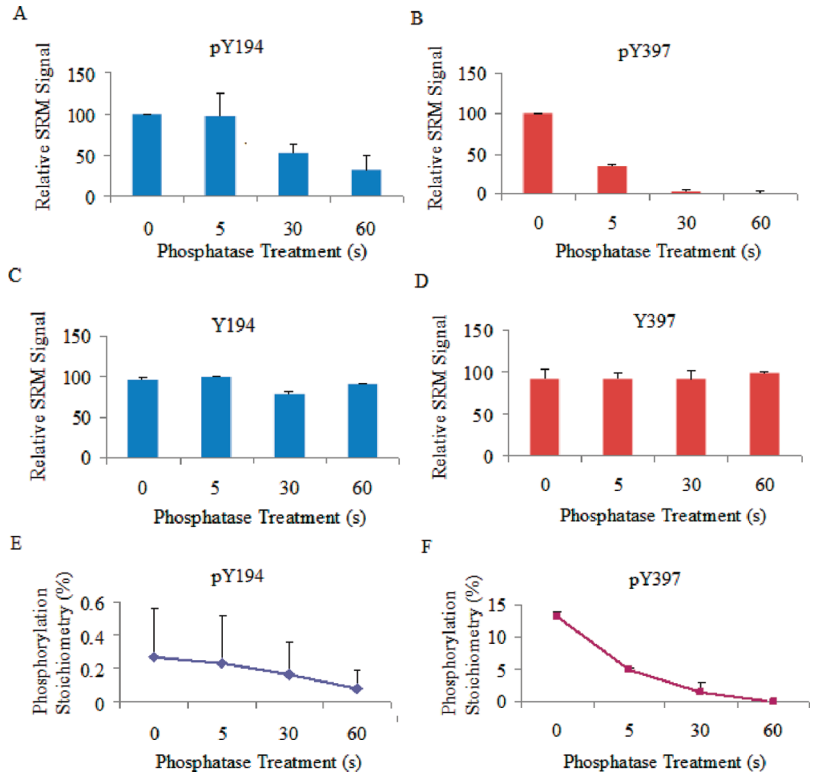

Figure 6. Determination of phosphorylation stoichiometry of Y194 and Y397 sites in GST Lyn fusion protein. (A−D), Bar graph of SRM signals (summed from SRM transitions listed in Table 1) of Lyn pY194 (A), pY397 (B), Y194 (C), and Y397 (D) -containing peptides normalized to the highest value of the perspective peptide; GST Lyn fusion protein was purified from bacteria, digested to peptides with trypsin, incubated with phosphatase (Calf Intestinal Alkaline Phosphatase 1 u) for indicated time, and analyzed by LC−SRM. (E and F) Calculated phosphorylation stoichiometry of Lyn Y194 (E) and Y397 (F) sites were plotted for indicated time. Error bars denote standard deviation in the results of two independent experiments.

but less than 0.3% at Y194. This is consistent with Y397 being a preferred autophosphorylation site. The low extent of the phosphorylation, as determined, confirmed the earlier speculation that these sites have low phosphorylation stoichiometries. It also demonstrated that the LC−SRM-based quantification assay was sensitive in that small changes in phosphorylation at a low stoichiometry (<1%) site (Y194) were clearly detected.

Measurement of Lyn Phosphorylation Stoichiometry in Multiple Myeloma Tumor Samples. To test our approach on tumor tissue, the MM cell line KMS12 was injected into mice to produce xenograft tumors. A sample of the tumor, and KMS12 cultured cells treated with or without pervanadate were lysed and enriched for Lyn by IP. The enriched fractions were protease digested and analyzed by LC−SRM. Transitions defining Y397-containing tryptic peptides in phosphorylated or unphosphorylated isoforms were measured (Figure 7A−C left panels). Peptide identities were manually confirmed by the coelution of the associated transitions. In every case, a major SRM signal (of summed transitions) was observed for the target peptide. In KMS12 cells without or with pervanadate and in the KMS12 tumor, the respective Y397 phosphorylation stoichiometries were 0.5 ± 0.7%, 52.4 ± 1.46%, and 3.2 ± 0.66% (±SD, $n = 3$; Figure 7D). In these samples, only nonphosphorylated Y194 peptides were detected, so the phosphorylation stoichiometry at Y194 was deemed too low to be determined (not determined, ND). We note that only approximately one-fifth the amount of cell/tissue lysate protein was used in this analysis compared with the experiment described above wherein the phosphorylation stoichiometry at Y194 was measured as 9.2% in pervanadate-treated KMS12.

To verify the quantification results for Y397 phosphorylation, the amount of Lyn protein and pY397 levels were examined in KMS12 cells and xenograft tumors by Western immunoblotting (Figure 7E). Compared to the untreated cells, the amounts of pY397 were approximately 39-fold and 8-fold higher in pervanadate treated cells and xenograft tumor, respectively. These findings approximated the SRM results of 100-fold and 6-fold, respectively.

Discussion

By combining the specificity of LC−SRM for targeted analysis of low-abundance phosphopeptides with label-free quantification, we demonstrated that the relative phosphorylation stoichiometry of the Lyn kinase can be determined in mammalian cells and tumor tissues. We measured the phosphorylation stoichiometry at Lyn Y397 in xenograft MM tumor tissue and demonstrated that the result is consistent with Western immuno blotting.

Compared to traditional antibody-based quantification methods[34,35] for phosphorylation stoichiometry determination, our approach has the advantage that it does not require site-specific antibodies. Therefore, it can be used to analyze the ever-growing population of novel phosphorylation sites and help to determine their biological functions. In addition, because response rate ratios remain constant under controlled experimental conditions, once the transitions are optimized and the response rate ratios defined, they can be repeatedly used to analyze multiple samples. Triple quadrupole MS instruments such as those used in this study can be configured

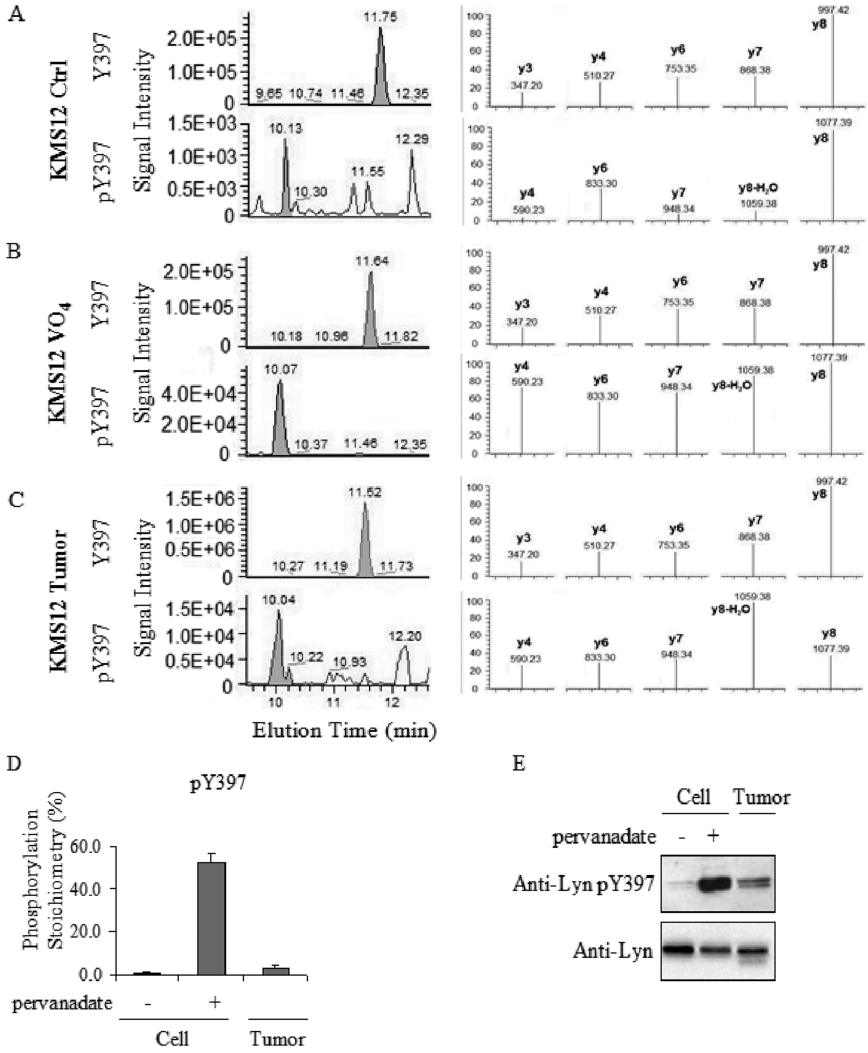

Figure 7. Lyn Y397 phosphorylation stoichiometry determination in KMS12 cells and xenograft tumor. (A−C) Summed signal peak (left, shaded) of SRM transitions (right) coeluted in one chromatographic peak corresponding to Lyn Y397 (top) and pY397 (bottom) -containing tryptic peptides. The peptides were derived from Lyn enriched fractions of KMS12 cells (A), KMS12 cells treated with pervanadate (B), and a xenograft tumor (C). (D) Bar graph of pY397 stoichiometries in KMS12 cells and tumor. Error bars indicate standard deviations ($n = 3$). (E) Lyn-enriched fractions of KMS12 control cells (left lane), cells treated with pervanadate (middle lane), and xenograft tumor (right lane) were blotted with an anti-Lyn-pY397 antibody (top) and anti-Lyn antibody (bottom).

to effectively monitor multiple (e.g., >100) transitions across an LC gradient. Therefore, it is conceivable that in a single multiplexed LC−SRM run (approximately 1 h machine time), relative stoichiometries for numerous phosphorylation sites may be obtained.

In the KMS11 and KMS12 myeloma cells, phosphorylation at Y397 in the kinase domain was sensitive to pervanadate treatment, indicating that the accumulation of (auto)phosphorylation at this site is constrained by cellular PTP activities. By contrast, PTP inhibition by pervanadate caused an accumulation of phosphorylation at Lyn Y194 only in KMS12, but not KMS11. This suggests KMS11 cells lack Lyn Y194 kinase activity relative to KMS12. KMS11 expresses the receptor tyrosine kinase fibroblast growth factor receptor-3 (FGFR3), which is a validated drug target in MM tumors (such as KMS11) that harbor the t(4;14) translocation.[36] By contrast, activated and/or overexpressed Y kinases have not been identified in KMS12 or most other non-t(4;14) myelomas. Our data indicate that Lyn should be examined further as a candidate activated Y kinase in KMS12 cells as a function of the potentially activating phosphorylation at Y194.

It remains a challenge to quantify pY sites associated with low stoichiometry, low-abundance proteins, or peptides with poor response rates.[37] By combining the specificity of LC−SRM for targeted analysis of low-abundance phosphopeptides with label-free quantification, we demonstrated that relative phosphorylation stoichiometry in the Lyn kinase can be determined in tumor-derived cells and tissue. This approach enabled the quantification of relative phosphorylation stoichiometries at less than 1% and over a range of at least 2 orders of magnitude. With this label-free approach, more accurate information about the signaling pathways in normal and diseased tissue may be retrieved and compared. This, in turn, may prove invaluable in identifying drug targets and devising novel diagnostic or treatment strategies.

Acknowledgment. This research was supported by funding to MFM from the Canada Research Chairs program, the Canadian Institutes of Health Research, and the Canadian Cancer Society Research Institute. We thank Dr. Ben Neel (Ontario Cancer Institute) for the generous gift of the PTP1B construct.

Supporting Information Available: Supplementary SI Figure 1, MS/MS spectra of Lyn-derive peptides identified by LC−MS/MS analysis; SI Figure 2, enzymatic activity of PTP1B examined in a dephosphorylation assay; SI Figure 3, assessment of Lyn-derived peptides as reference peptides for normalization; Supplementary Si Table 1, properties of Lyn-derived peptides detected by LC−MS and monitored by SRM; and Supplementary Methods. This material is available free of charge via the Internet at http://pubs.acs.org.

References

(1) Zhang, J.; Yang, P. L.; Gray, N. S. Targeting cancer with small molecule kinase inhibitors. *Nat. Rev. Cancer* **2009**, *9* (1), 28–39.

(2) Moran, M. F.; Tong, J.; Taylor, P.; Ewing, R. M. Emerging applications for phospho-proteomics in cancer molecular therapeutics. *Biochim. Biophys. Acta* **2006**, *1766* (2), 230–41.

(3) Olsen, J. V.; Blagoev, B.; Gnad, F.; Macek, B.; Kumar, C.; Mortensen, P.; Mann, M. Global, in vivo, and site-specific phosphorylation dynamics in signaling networks. *Cell* **2006**, *127* (3), 635–48.

(4) Macek, B.; Mann, M.; Olsen, J. V. Global and site-specific quantitative phosphoproteomics: principles and applications. *Annu. Rev. Pharmacol. Toxicol.* **2009**, *49*, 199–221.

(5) Thingholm, T. E.; Jensen, O. N.; Larsen, M. R. Analytical strategies for phosphoproteomics. *Proteomics* **2009**, *9* (6), 1451–68.

(6) Aebersold, R.; Mann, M. Mass spectrometry-based proteomics. *Nature* **2003**, *422* (6928), 198–207.

(7) Stover, D.; Caldwell, J.; Marto, J.; Root, K.; Mestan, J.; Stumm, M.; Ornatsky, O.; Orsi, C.; Radosevic, N.; Liao, L.; Fabbro, D.; Moran, M. F. Differential phosphoprofiles of EGF and EGFR kinase inhibitor-treated human tumor cells and mouse xenografts. *Clin. Proteomics* **2004**, *1* (1), 69–80.

(8) Steen, H.; Jebanathirajah, J. A.; Springer, M.; Kirschner, M. W. Stable isotope-free relative and absolute quantitation of protein phosphorylation stoichiometry by MS. *Proc. Natl. Acad. Sci. U.S.A.* **2005**, *102* (11), 3948–53.

(9) Wang, M.; You, J.; Bemis, K. G.; Tegeler, T. J.; Brown, D. P. Label-free mass spectrometry-based protein quantification technologies in proteomic analysis. *Briefings Funct. Genomics Proteomics* **2008**, *7* (5), 329–39.

(10) Wang, G.; Wu, W. W.; Zeng, W.; Chou, C. L.; Shen, R. F. Label-free protein quantification using LC-coupled ion trap or FT mass spectrometry: Reproducibility, linearity, and application with complex proteomes. *J. Proteome Res.* **2006**, *5* (5), 1214–23.

(11) Mueller, L. N.; Brusniak, M. Y.; Mani, D. R.; Aebersold, R. An assessment of software solutions for the analysis of mass spectrometry based quantitative proteomics data. *J. Proteome Res.* **2008**, *7* (1), 51–61.

(12) Tong, J.; Taylor, P.; Peterman, S. M.; Prakash, A.; Moran, M. F. Epidermal growth factor receptor phosphorylation sites Ser991 and Tyr998 are implicated in the regulation of receptor endocytosis and phosphorylations at Ser1039 and Thr1041. *Mol. Cell. Proteomics* **2009**, *8* (9), 2131–44.

(13) Steen, J. A.; Steen, H.; Georgi, A.; Parker, K.; Springer, M.; Kirchner, M.; Hamprecht, F.; Kirschner, M. W. Different phosphorylation states of the anaphase promoting complex in response to antimitotic drugs: a quantitative proteomic analysis. *Proc. Natl. Acad. Sci. U.S.A.* **2008**, *105* (16), 6069–74.

(14) Wang, J.; Jiang, Y.; Wang, Y.; Zhao, X.; Cui, Y.; Gu, J. Liquid chromatography tandem mass spectrometry assay to determine the pharmacokinetics of aildenafil in human plasma. *J. Pharm. Biomed. Anal.* **2007**, *44* (1), 231–5.

(15) Hartmann, S.; Okun, J. G.; Schmidt, C.; Langhans, C. D.; Garbade, S. F.; Burgard, P.; Haas, D.; Sass, J. O.; Nyhan, W. L.; Hoffmann, G. F. Comprehensive detection of disorders of purine and pyrimidine metabolism by HPLC with electrospray ionization tandem mass spectrometry. *Clin. Chem.* **2006**, *52* (6), 1127–37.

(16) Nirogi, R. V.; Kandikere, V. N.; Shukla, M.; Mudigonda, K.; Shrivasthava, W.; Datla, P. V.; Yerramilli, A. Simultaneous quantification of cilostazol and its primary metabolite 3,4-dehydrocilostazol in human plasma by rapid liquid chromatography/tandem mass spectrometry. *Anal. Bioanal. Chem.* **2006**, *384* (3), 780–90.

(17) Rifai, N.; Gillette, M. A.; Carr, S. A. Protein biomarker discovery and validation: the long and uncertain path to clinical utility. *Nat. Biotechnol.* **2006**, *24* (8), 971–83.

(18) Ciccimaro, E.; Hanks, S. K.; Yu, K. H.; Blair, I. A. Absolute quantification of phosphorylation on the kinase activation loop of cellular focal adhesion kinase by stable isotope dilution liquid chromatography/mass spectrometry. *Anal. Chem.* **2009**, *81* (9), 3304–13.

(19) Mayya, V.; Rezual, K.; Wu, L.; Fong, M. B.; Han, D. K. Absolute quantification of multisite phosphorylation by selective reaction monitoring mass spectrometry: determination of inhibitory phosphorylation status of cyclin-dependent kinases. *Mol. Cell. Proteomics* **2006**, *5* (6), 1146–57.

(20) Glinski, M.; Weckwerth, W. Differential multisite phosphorylation of the trehalose-6-phosphate synthase gene family in Arabidopsis thaliana: a mass spectrometry-based process for multiparallel peptide library phosphorylation analysis. *Mol. Cell. Proteomics* **2005**, *4* (10), 1614–25.

(21) Wolf-Yadlin, A.; Hautaniemi, S.; Lauffenburger, D. A.; White, F. M. Multiple reaction monitoring for robust quantitative proteomic analysis of cellular signaling networks. *Proc. Natl. Acad. Sci. U.S.A.* **2007**, *104* (14), 5860–5.

(22) Steen, H.; Jebanathirajah, J. A.; Rush, J.; Morrice, N.; Kirschner, M. W. Phosphorylation analysis by mass spectrometry: myths, facts, and the consequences for qualitative and quantitative measurements. *Mol. Cell. Proteomics* **2006**, *5* (1), 172–81.

(23) Marcantonio, M.; Trost, M.; Courcelles, M.; Desjardins, M.; Thibault, P. Combined enzymatic and data mining approaches for comprehensive phosphoproteome analyses: application to cell signaling events of interferon-gamma-stimulated macrophages. *Mol. Cell. Proteomics* **2008**, *7* (4), 645–60.

(24) Smith, J. R.; Olivier, M.; Greene, A. S. Relative quantification of peptide phosphorylation in a complex mixture using 18O labeling. *Physiol. Genomics* **2007**, *31* (2), 357–63.

(25) Xu, Y.; Harder, K. W.; Huntington, N. D.; Hibbs, M. L.; Tarlinton, D. M. Lyn tyrosine kinase: accentuating the positive and the negative. *Immunity* **2005**, *22* (1), 9–18.

(26) Stover, D. R.; Furet, P.; Lydon, N. B. Modulation of the SH2 binding specificity and kinase activity of Src by tyrosine phosphorylation within its SH2 domain. *J. Biol. Chem.* **1996**, *271* (21), 12481–7.

(27) Tong, J.; Taylor, P.; Jovceva, E.; St-Germain, J. R.; Jin, L. L.; Nikolic, A.; Gu, X.; Li, Z. H.; Trudel, S.; Moran, M. F. Tandem immunoprecipitation of phosphotyrosine-mass spectrometry (TIPY-MS) indicates C19ORF19 becomes tyrosine-phosphorylated and associated with activated epidermal growth factor receptor. *J. Proteome Res.* **2008**, *7* (3), 1067–77.

(28) Craig, R.; Beavis, R. C. TANDEM: matching proteins with tandem mass spectra. *Bioinformatics* **2004**, *20* (9), 1466–7.

(29) Mueller, L. N.; Rinner, O.; Schmidt, A.; Letarte, S.; Bodenmiller, B.; Brusniak, M. Y.; Vitek, O.; Aebersold, R.; Muller, M. SuperHirn - a novel tool for high resolution LC-MS-based peptide/protein profiling. *Proteomics* **2007**, *7* (19), 3470–80.

(30) Prakash, A.; Tomazela, D. M.; Frewen, B.; Maclean, B.; Merrihew, G.; Peterman, S.; Maccoss, M. J. Expediting the development of targeted SRM assays: using data from shotgun proteomics to automate method development. *J. Proteome Res.* **2009**, *8* (6), 2733–9.

(31) Hallek, M.; Neumann, C.; Schaffer, M.; Danhauser-Riedl, S.; von Bubnoff, N.; de Vos, G.; Druker, B. J.; Yasukawa, K.; Griffin, J. D.; Emmerich, B. Signal transduction of interleukin-6 involves tyrosine phosphorylation of multiple cytosolic proteins and activation of Src-family kinases Fyn, Hck, and Lyn in multiple myeloma cell lines. *Exp. Hematol.* **1997**, *25* (13), 1367–77.

(32) Sicheri, F.; Kuriyan, J. Structures of Src-family tyrosine kinases. *Curr. Opin. Struct. Biol.* **1997**, *7* (6), 777–85.

(33) Rush, J.; Moritz, A.; Lee, K. A.; Guo, A.; Goss, V. L.; Spek, E. J.; Zhang, H.; Zha, X. M.; Polakiewicz, R. D.; Comb, M. J. Immunoaffinity profiling of tyrosine phosphorylation in cancer cells. *Nat. Biotechnol.* **2005**, *23* (1), 94–101.

(34) Gembitsky, D. S.; Lawlor, K.; Jacovina, A.; Yaneva, M.; Tempst, P. A prototype antibody microarray platform to monitor changes in protein tyrosine phosphorylation. *Mol. Cell. Proteomics* **2004**, *3* (11), 1102–18.

(35) Tkaczyk, C.; Metcalfe, D. D.; Gilfillan, A. M. Determination of protein phosphorylation in Fc epsilon RI-activated human mast cells by immunoblot analysis requires protein extraction under denaturing conditions. *J. Immunol. Methods* **2002**, *268* (2), 239–43.

(36) Trudel, S.; Ely, S.; Farooqi, Y.; Affer, M.; Robbiani, D. F.; Chesi, M.; Bergsagel, P. L. Inhibition of fibroblast growth factor receptor 3 induces differentiation and apoptosis in t(4;14) myeloma. *Blood* **2004**, *103* (9), 3521–8.

(37) Mann, M.; Ong, S. E.; Gronborg, M.; Steen, H.; Jensen, O. N.; Pandey, A. Analysis of protein phosphorylation using mass spectrometry: deciphering the phosphoproteome. *Trends Biotechnol.* **2002**, *20* (6), 261–8.

PR100024A